



CHORUS

This is the accepted manuscript made available via CHORUS. The article has been published as:

Extreme multistability in a chemical model system

Calistus N. Ngonghala, Ulrike Feudel, and Kenneth Showalter

Phys. Rev. E **83**, 056206 — Published 9 May 2011

DOI: [10.1103/PhysRevE.83.056206](https://doi.org/10.1103/PhysRevE.83.056206)

Extreme Multistability in a Chemical Model System

Calistus N. Ngonghala¹, Ulrike Feudel² and Kenneth Showalter³

¹*Department of Mathematics, West Virginia University,
Morgantown, West Virginia 26506-6310*

²*Theoretical Physics/Complex Systems, ICBM,
Carl von Ossietzky University Oldenburg,
PF 2503, 26111 Oldenburg, Germany and*

³*Department of Chemistry,
West Virginia University, Morgantown,
West Virginia 26506-6045*

Abstract

Coupled systems can exhibit an unusual kind of multistability, namely the coexistence of infinitely many attractors for a given set of parameters. This extreme multistability is demonstrated to occur in coupled chemical model systems with various types of coupling. We show that the appearance of extreme multistability is associated with the emergence of a conserved quantity in the long-term limit. This conserved quantity leads to a “slicing” of the state space into manifolds corresponding to the value of the conserved quantity. The state space “slices” develop as $t \rightarrow \infty$ and there exists at least one attractor in each of them. We discuss the dependence of extreme multistability on the coupling and on the mismatch of parameters of the coupled systems.

PACS numbers: PACS numbers: 05.45.-a

I. INTRODUCTION

Nonlinear dynamical systems exhibit a rich variety of long-term behaviors, such as stationary points, periodic and quasiperiodic oscillations, and chaotic behavior. Various bifurcations and transitions are known, and their dependence on one or more control parameters provides a characterization of the complex dynamics of a system [1, 2]. Most of the work devoted to dynamical systems theory deals with systems having one or only a few attractors for a given set of parameters. However, many physical and biological systems are known in which there are a multitude of coexisting attractors [3–5]. Examples include systems from laser physics [6, 7], semiconductor physics [8, 9], chemistry [10, 11], neuroscience [12], and population dynamics [13]. Multistability is, in fact, a rather common phenomenon that is found in completely different classes of systems, such as weakly dissipative systems [14, 15], coupled systems [16–18], and systems with time delay [19–21].

An example of extreme multistability, a system with an infinite number of coexisting attractors, was reported by Sun et al. [22]. Two coupled Lorenz systems were studied, in which all parameters of the coupled system were held fixed and only the initial conditions were varied. Changes in initial conditions or perturbations cause the system to evolve to completely new attractors with different statistical properties. Consequently, such systems exhibit an infinite number of asymptotic attractors, some stationary, some periodic and some chaotic. The complexity of the behavior is visualized by plotting the long-term attractors versus the initial conditions in simulations. Surprisingly, these plots closely resemble bifurcation diagrams; however, the initial conditions can not be regarded as a bifurcation parameter. Moreover, all of the transitions between different attractors can be observed by simply varying the initial value of one of the state variables.

Chemical systems are among the most studied examples of dynamical systems exhibiting complex behavior, chaos and pattern formation [23, 24]. The dynamics giving rise to extreme multistability might account for reported irreproducibility of behavior in the chlorate-thiosulfate reaction [25] and in the chlorite-iodide reaction [26]. In both of these reactions, the behavior varies from experiment to experiment under the same set of experimental conditions. The inability to reproduce the dynamical behavior for the same set of conditions, despite care to ensure reproducibility, suggests that the inherent dynamics of these systems is playing some role. In a modified three-variable autocatalator model, Wang et al. [27] showed that this system can possess infinitely many

coexisting attractors when a “buffer step” is included in the chemical kinetics, where two reactants are produced and consumed in the same processes, a mechanism similar to that proposed by Epstein and co-workers for the chlorate-thiosulfate and chlorite-iodide reactions [25, 26].

In this paper, we investigate two coupled chemical systems, each possessing an infinite number of coexisting attractors. In contrast to the autocatalator model studied in [27], the extreme multistability arises from the coupling of two subsystems. We show how the coupling, in two different schemes, yields extreme multistability behavior. In both cases, this phenomenon is associated with the generalized synchronization of the two coupled subsystems as well as the emergence of a conserved quantity. In the first coupling scheme, the conserved quantity is determined by a conservation law of all intermediate species, weighted by their reaction time constants, and is therefore given by the initial concentrations of these intermediates. For the second coupling scheme, this conserved quantity appears dynamically in the long-term limit as $t \rightarrow \infty$, and the dependence on initial conditions is therefore more complex. We show in both cases that, due to the presence of a conserved quantity, the state space is divided into submanifolds, each with an attractor associated with the value of the conserved quantity. Since the conserved quantity can take any real value, we obtain infinitely many attractors.

The paper is organized as follows: We begin with a review of the three-variable autocatalator model in Section II and present an analysis of its qualitative behavior. We then describe the coupling of two three-variable autocatalator systems to yield a six-variable autocatalator system in Section III, where we show that the coupled system exhibits extreme multistability characterized by a conserved quantity. We also show that the two subsystems exhibit generalized synchronization similar to lag synchronization. In Section IV, we check the robustness of the phenomenon of extreme multistability by introducing another coupling scheme. We again find generalized synchronization between the two subsystems but now characterized by complete synchronization between two pairs of the corresponding variables of the subsystems, while the difference in the third pair obeys a certain constant. This also leads to the appearance of an infinite number of synchronization manifolds. The emerging conserved quantity that defines the synchronization manifold can be used to reduce the six-dimensional system to a three-dimensional system without loss of generality. In addition, we study the robustness of the phenomenon of extreme multistability with respect to a mismatch of the parameters of the two subsystems, making them non-identical. Finally we discuss our results in Section V.

II. THE THREE-VARIABLE AUTOCATALATOR MODEL

Our investigation is based on a chemical model system that has been used in various studies of chemical oscillations and chaotic dynamics [28–33]. The three-variable autocatalator [34] is based on a two-variable version originally introduced by Gray & Scott [35], which has been used in many studies of the dynamics of chemical oscillations (cf. [36, 37] for details). Unlike the two-variable autocatalator, the three-variable model incorporates a second feedback loop and, hence, is capable of exhibiting complex periodic behavior as well as chaos. The model reaction scheme involves the conversion of a precursor reactant A with constant concentration to a final product B via three intermediates, X , Y and Z . The six reaction steps of the scheme, with rate constants k_i ($i = 0, \dots, 5$), are



The fourth reaction (R_4) in the above system describes an autocatalytic process whereby the intermediate species Y catalyzes its own production. This autocatalysis introduces a nonlinear reaction term that is essential for the oscillatory behavior of the system [35]. The chaotic behavior arises as a result of a second feedback loop through the variable Z in (R_5). Notice that Z is produced from this reaction and fed back into the system through reaction (R_2) to catalyze the production of X from A . Unlike reaction (R_4), in which Y is an autocatalyst, Z serves as a simple catalyst in reaction (R_2).

Letting A_0 , $[X]$, $[Y]$ and $[Z]$ be the concentrations of A , X , Y and Z , we write the following rate equations for the time evolution of the variable species:

$$\begin{aligned} \dot{[X]} &= k_0 A_0 + k_1 A_0 [Z] - k_2 [X] - k_3 [X][Y]^2, \\ \dot{[Y]} &= k_2 [X] + k_3 [X][Y]^2 - k_4 [Y], \\ \dot{[Z]} &= k_4 [Y] - k_5 [Z], \end{aligned} \quad (\text{II.1})$$

where the concentration of the precursor A is held constant at A_0 . Using the dimensionless variables

$$x = \left(\frac{k_3 k_2}{k_4^2} \right)^{\frac{1}{2}} [X], \quad y = \left(\frac{k_3}{k_2} \right)^{\frac{1}{2}} [Y], \quad z = \left(\frac{k_3 k_5^2}{k_2 k_4^2} \right)^{\frac{1}{2}} [Z], \quad \tau = k_2 t,$$

and the positive dimensionless parameters

$$\mu = \left(\frac{k_1}{k_5} \right) A_0, \quad \kappa = \left(\frac{k_0 k_5}{k_1 k_4} \right) \left(\frac{k_3}{k_2} \right)^{\frac{1}{2}}, \quad \sigma = \left(\frac{k_2}{k_4} \right), \quad \delta = \left(\frac{k_2}{k_5} \right),$$

we obtain the following scaled rate equations [38]:

$$\begin{aligned} \dot{x} &= \mu(\kappa + z) - x(1 + y^2), \\ \sigma \dot{y} &= x(1 + y^2) - y, \\ \delta \dot{z} &= y - z. \end{aligned} \tag{II.2}$$

Since σ and δ denote time scales, these parameters are positive, and the same applies to κ , which is a combination of reaction rate constants. The parameter that is naturally varied is $\mu \geq 0$, which is a function of the constant concentration A_0 of the precursor reactant. Hence, μ serves as a bifurcation parameter that allows examination of the transitions between different dynamical behaviors.

Let us briefly recall the dynamics of the system and its dependence on the parameters (cf. [28] for details). We will vary only μ in the interval $0 \leq \mu < 1$, while holding constant the parameters $\kappa = 65$, $\sigma = 5 \times 10^{-3}$ and $\delta = 2 \times 10^{-2}$. As μ is gradually increased, a number of different dynamical behaviors are observed. We obtain a stable steady state for $0 \leq \mu < 0.016$, a Hopf bifurcation occurs at $\mu = 0.016$ leading to oscillatory behavior, and this is followed by the first period doubling at $\mu = 0.143$ and the second period doubling at $\mu = 0.153$. The subsequent period doubling cascade ends in a transition to chaos at $\mu \simeq 0.154$. Further increases of μ lead to a bifurcation sequence from chaos via an inverse period doubling cascade and a second Hopf bifurcation at $\mu = 0.175$ back to a steady state. Figure 1 shows the bifurcation diagram for system (II.2).

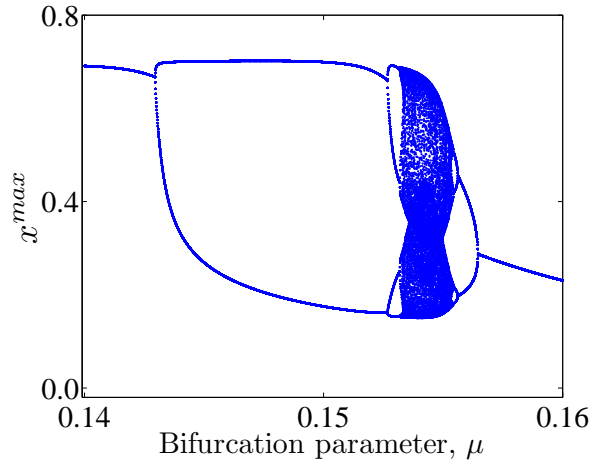


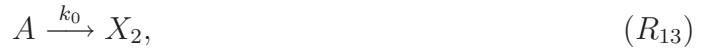
FIG. 1: (Color online) Bifurcation diagram of the three-variable autocatalator model. The maximum amplitude of x is plotted as a function of the bifurcation parameter μ showing a period doubling sequence, chaos and a reverse period doubling sequence.

We note that the three-variable autocatalator model possesses a unique attractor for all values of the bifurcation parameter μ we consider, i.e., all initial conditions converge to a specific attractor for each value of μ . In other words, there is no sign of multistability corresponding to coexisting attractors for any parameter set considered here.

III. TWO COUPLED AUTOCATALATOR MODELS

The dynamical behavior becomes much more complex when two three-variable autocatalator models are coupled in a particular way. To achieve this coupling, we consider two autocatalator subsystems with variables X_1, Y_1, Z_1 and X_2, Y_2, Z_2 in which the coupling is realized through Z_2 in the second equation of the first subsystem (R_8) and indirectly through Z_1 in the sixth equation of the second subsystem (R_{18}), since the reactant E is produced from Z_1 in the first subsystem

(R₁₂). The coupling of the autocatalator subsystems is shown by the following chemical reactions:



Assuming that $k'_5 \gg k_5$, we formulate the following dimensionless rate equations:

$$\begin{aligned} \dot{x}_1 &= \mu(\kappa + z_2) - x_1(1 + y_1^2), \\ \sigma \dot{y}_1 &= x_1 - y_1 + x_1 y_1^2, \\ \delta \dot{z}_1 &= y_1 - z_1, \\ \dot{x}_2 &= \mu(\kappa + z_2) - x_2(1 + y_2^2), \\ \sigma \dot{y}_2 &= x_2 - y_2 + x_2 y_2^2, \\ \delta \dot{z}_2 &= y_2 - z_1, \end{aligned} \quad (\text{III.1})$$

where $\tau = k_2 t$, $x_1 = \frac{(k_1 k_3)^{\frac{1}{2}}}{k_4} [X_1]$, $y_1 = \left(\frac{k_3}{k_2}\right)^{\frac{1}{2}} [Y_1]$, $z_1 = \left(\frac{k_5}{k_4}\right) \left(\frac{k_3}{k_2}\right)^{\frac{1}{2}} [Z_1]$,

$$x_2 = \frac{(k_1 k_3)^{\frac{1}{2}}}{k_4} [X_2], \quad y_2 = \left(\frac{k_3}{k_2}\right)^{\frac{1}{2}} [Y_2], \quad z_2 = \left(\frac{k_5}{k_4}\right) \left(\frac{k_3}{k_2}\right)^{\frac{1}{2}} [Z_2], \quad \mu = \frac{k_1 A_0}{k_5},$$

$$\kappa = \left(\frac{k_0 k_5}{k_1 k_4}\right) \left(\frac{k_3}{k_2}\right)^{\frac{1}{2}}, \quad \sigma = \frac{k_2}{k_4} \text{ and } \delta = \frac{k_2}{k_5}.$$

While the dynamics of a single subsystem possesses a unique attractor as discussed in Sec. II, we now observe a multitude of coexisting attractors. Specifically, the coupled system exhibits extreme multistability, i.e., an infinite number of attractors exists for a given set of parameters.

To demonstrate this behavior, we fix the parameters such that the uncoupled three-variable autocatalator exhibits a simple periodic solution ($\mu = 0.157$, $\kappa = 65$, $\sigma = 5 \times 10^{-3}$, $\delta = 2 \times 10^{-2}$), which is established from any set of initial conditions in the three-dimensional state space. Let us now investigate the final state to which the coupled autocatalator system converges, where only positive initial conditions are permitted, since the six variables correspond to chemical concentrations. We proceed by fixing five out of six of the initial conditions, $(0.01, 0.1, 0.1, 0.0, y_{02}, 0.0)$, and varying the initial value of y_2 within the interval $4.0 \leq y_{02} \leq 8$. We then integrate the system using a fourth-order Runge-Kutta method with variable step size [39]. In order to ensure that asymptotic behavior is exhibited, the simulations were carried out for at least 10,000 time steps, and only the last one-tenth of each time series was used. Identical behavior was found in simulations with one-half and three-quarters as many time steps, showing that the behavior is asymptotic. We also employed higher-order Runge-Kutta methods (7th-8th order) to verify the accuracy of our results.

We find a wide variety of dynamics, ranging from simple periodic motion for large values of y_{02} to oscillations of different periods for intermediate values to chaotic behavior for small values of y_{02} . This behavior is shown in Fig. 2, which depicts the maximum values of the amplitude of x_1 (corresponding to a Poincaré section) so that a simple oscillation of period T appears as a fixed point. In fact, the picture we obtain appears much like a complete bifurcation diagram for an inverse period-doubling cascade. However, since we do not change any bifurcation parameters but only the initial conditions, it only resembles a bifurcation diagram. Period doubling is found at $y_{02} = 7.145$ ($T \rightarrow 2T$), $y_{02} = 5.515$ ($2T \rightarrow 4T$), $y_{02} = 5.165$ ($4T \rightarrow 8T$), and $y_{02} = 5.095$ ($8T \rightarrow 16T$). Chaotic behavior immersed with periodic windows is evident as well.

One could argue that the number of attractors is finite because there are entire intervals of y_{02} leading to an oscillation of a certain period, for example, period $2T$. However, for each initial condition within this interval, the location of the $2T$ periodic orbit is slightly different. This means that for any pair of nearby initial conditions the corresponding final states are never identical. In this sense, we obtain an infinite number of quantitatively different attractors in state space. In addition, since the period doubling cascade is complete, we also know that an infinite number of qualitatively different attractors coexist.

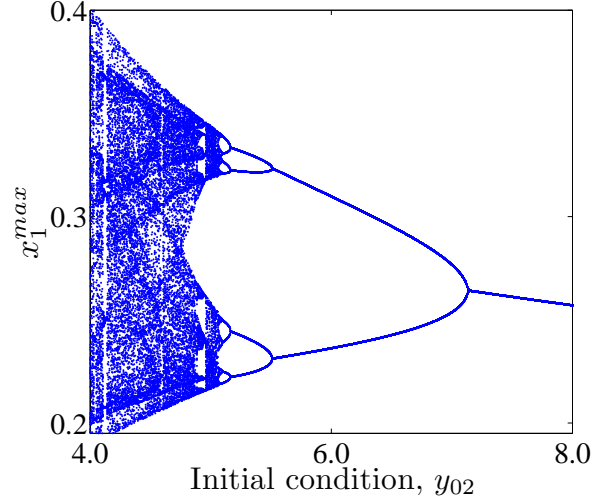


FIG. 2: (Color online) Long-term dynamics of the coupled six-variable autocatalator model. A plot of the maximum amplitude of x_1 as a function of the initial condition y_{02} .

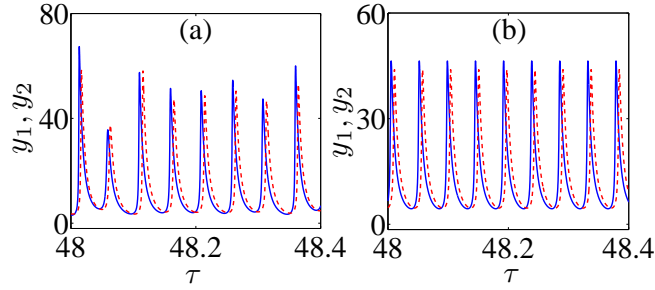


FIG. 3: (Color online) Time series plots illustrating the differences between y_1 and y_2 within the chaotic and period-1 regimes. (a) Chaotic regime, $y_{02} = 4.5$, and (b) period-1 regime, $y_{02} = 7.5$, with solid blue lines showing y_1 and broken red lines showing y_2 . Similar differences are observed between x_1 and x_2 and z_1 and z_2 .

To explain the appearance of extreme multistability, we note that the coupling scheme between the two subsystems, (R_7) - (R_{12}) and (R_{13}) - (R_{18}) , gives rise to a conserved quantity. This quantity, which we call C with $dC/dt = 0$, corresponds to the difference between the concentrations of the intermediate species in each subsystem weighted by their reaction time constants:

$$C = x_2 + \sigma y_2 + \delta z_2 - (x_1 + \sigma y_1 + \delta z_1). \quad (\text{III.2})$$

Using Eqs. (III.1), it is easy to show that the conservation condition $dC/dt = 0$ is always fulfilled. The value of C , given by the initial condition $C = x_{02} + \sigma y_{02} + \delta z_{02} - (x_{01} + \sigma y_{01} + \delta z_{01})$, defines a complex manifold in state space on which the dynamics takes place. Based on the existence of the conserved quantity C , we illustrate the extreme multistability with a schematic representation, depicted in Fig. 4. The entire state space is densely filled with manifolds (hypersurfaces) that are defined by the quantity C . In each of these manifolds there exists at least one attractor. Since C can take any real value, the state space is “sliced” into infinitely many such manifolds, with each containing a different long-term dynamics. Changing the initial conditions corresponds to a change of the manifold in which the dynamics takes place.

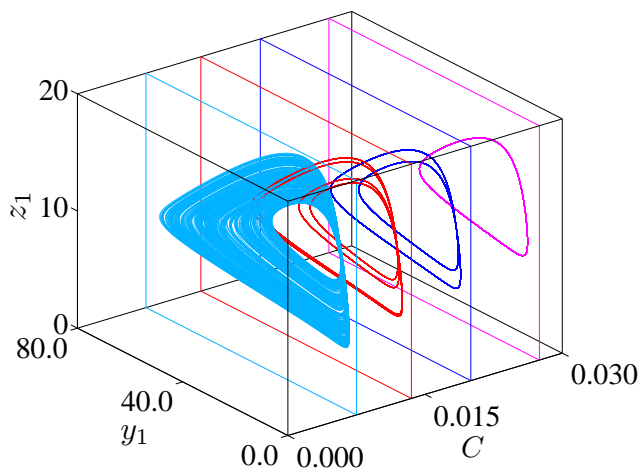


FIG. 4: (Color online) A sampling of the synchronization manifolds as a function of the conserved quantity C . Chaotic behavior (light blue), period-4 (red), period-2 (dark blue), and period-1 (magenta) are exhibited for $C = 0.0075, 0.0135, 0.0200,$ and 0.0275 .

Due to the existence of a conserved quantity, the dynamics becomes similar to the dynamics of Hamiltonian systems, where the marginally stable invariant set exhibited in the long-term limit depends on the value of the energy of the system. However, it is important to note that, in contrast to the Hamiltonian case, the coupled autocatalator system is dissipative, and the invariant sets exhibited in the long-term limit are attractors. As can be seen from the form of the conserved quantity C in Eq. (III.2), an infinite number of initial conditions give rise to a particular value and therefore a particular attractor.

Basins of attraction, i.e., the sets of initial conditions that all converge to the same attractor,

are an important concept in the study of multistable systems. In the case of extreme multistability, each of the attractors also has its own basin of attraction. This basin of attraction is given by all initial conditions fulfilling Eq. (III.2). The basin of attraction of each attractor is therefore the manifold determined by the particular value of the conserved quantity. However, these manifolds or slices in state space are dense, so that in each arbitrarily close neighborhood of each manifold there is another manifold leading to another attractor. This means that in each arbitrarily close neighborhood of an attractor there are points belonging to another manifold and, hence, to another basin of attraction. As a consequence, all attractors in our system are weak attractors in the Milnor sense [40].

The existence of a conserved quantity allows us to reduce the dimension of the dynamical system by one variable. Substituting z_2 from Eq. (III.2) into Eqs. (III.1) leads to

$$\begin{aligned}
\dot{x}_1 &= \mu(\kappa + (x_1 + \sigma y_1 + \delta z_1 + C - x_2 - \sigma y_2)/\delta) - x_1(1 + y_1^2), \\
\sigma \dot{y}_1 &= x_1 - y_1 + x_1 y_1^2, \\
\delta \dot{z}_1 &= y_1 - z_1, \\
\dot{x}_2 &= \mu(\kappa + (x_1 + \sigma y_1 + \delta y_1 - C - x_2 - \sigma y_2)/\delta) - x_2(1 + y_2^2), \\
\sigma \dot{y}_2 &= x_2 - y_2 + x_2 y_2^2.
\end{aligned}
\tag{III.3}$$

From this rewriting it becomes obvious that the conserved quantity C , and hence the initial condition y_{02} , can indeed be regarded as a bifurcation parameter in the reduced system (III.3), and Fig. 2 can therefore be interpreted as a bifurcation diagram, in the mathematical sense, exhibiting many known dynamical transitions.

The existence of the conserved quantity also appears when computing Lyapunov exponents to check for chaotic behavior, as shown in Fig. 5. For all initial conditions, we obtain two zero Lyapunov exponents, where the first zero is the usual one corresponding to the Lyapunov exponent along the trajectory, while the second zero corresponds to the existence of a conserved quantity.

Finally, we discuss the relation between the dynamics of the two coupled oscillators. As shown in Fig. 3(a), the two oscillators synchronize with a certain time lag so that the phase retains a fixed difference, while the amplitude difference varies. In Fig. 3(b), we see simple lag synchronization in the periodic case. It is important to note that lag synchronization generally emerges while varying the coupling strength between two oscillators [41]; however, such a change is not possible in this system, where the coupling is realized by chemical reactions. With this restriction in mind, we note

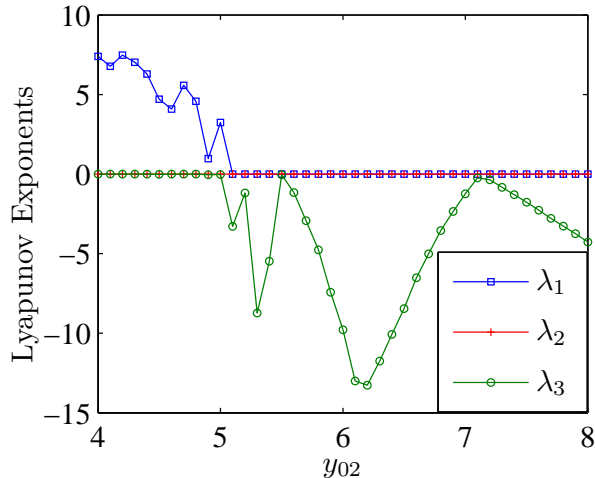


FIG. 5: (Color online) The three largest Lyapunov exponents of the coupled six-variable autocatalator model (III.1) as a function of the initial condition y_{02} .

that the coupled autocatalators exhibit a type of generalized synchronization with features much like those seen in chaotic synchronization.

IV. ROBUSTNESS OF EXTREME MULTISTABILITY

A. Second coupling scheme

In the previous section, we have shown that extreme multistability can emerge for two three-variable autocatalator systems coupled in a particular way. This coupling leads to the existence of a conserved quantity that appears in the model equations, suggesting that the phenomenon may be rather special and may not occur in any other case. Therefore, we now consider another coupling to demonstrate that different coupling schemes can give rise to extreme multistability. In contrast to the previously considered system, however, the conserved quantity associated with the phenomenon is not contained in the model equations but arises in a non-trivial way as a result of the system dynamics in the long-term limit. The coupling of the two autocatalator subsystems is more complex here than the first coupling scheme, and we describe the six-variable chemical model in the Appendix, Sec. VII.

We now turn to the dimensionless model system to demonstrate the extreme multistability and

present an analysis of the behavior. Using the same scaling as in the previous section, we obtain the following dimensionless system:

$$\begin{aligned}
 \dot{x}_1 &= \mu(\kappa + z_1) - x_1(1 + y_1^2), \\
 \sigma \dot{y}_1 &= x_1(1 + y_1^2) - y_1, \\
 \delta \dot{z}_1 &= y_2 - z_1, \\
 \dot{x}_2 &= \mu(\kappa + z_2) - x_2(1 + y_1^2), \\
 \sigma \dot{y}_2 &= x_2(1 + y_1^2) - y_2, \\
 \delta \dot{z}_2 &= y_2 - z_2.
 \end{aligned}
 \tag{IV.1}$$

As with first coupling scheme described by (R7)-(R18) and Eqs. (III.1), we use the parameters $\kappa = 65$, $\sigma = 5 \times 10^{-3}$ and $\delta = 2 \times 10^{-2}$. The bifurcation parameter is set to $\mu = 0.145$, which corresponds to period-2 behavior of the single uncoupled three-variable autocatalator. The coupled six-variable autocatalator exhibits the phenomenon of extreme multistability, as illustrated in Fig. 6, for the initial conditions $(0.01, 0.1, 0.1, 0, y_{02}, 0)$ with variable y_{02} .

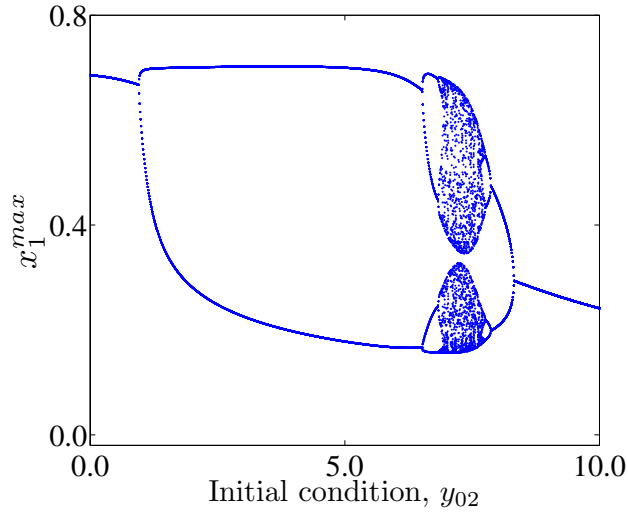


FIG. 6: (Color online) Long-term dynamics of the coupled six-variable autocatalator as a function of the initial condition y_{02} .

In contrast to the coupled autocatalator system described by Eqs. (III.1), the new coupling in Eqs. (IV.1) gives rise to a different generalized synchronization between the two subsystems, in

which two pairs of the variables, x_1, x_2 and z_1, z_2 , synchronize completely, while the third pair is determined by a constant difference, $c = y_2 - y_1$. Hence, the synchronization is associated with the emergence of a conserved quantity c that characterizes the synchronization manifold. Another difference from the system described by Eqs. (III.1) is that the conserved quantity c appears as a result of the system dynamics, and it takes its final value only in the long-term limit $t \rightarrow \infty$. To justify this statement, let us introduce the new variables $e_i, i = 1, 2, 3$, which are convenient for characterizing synchronization because they describe the deviations from complete synchronization [42]: $e_1 = x_2 - x_1, e_2 = y_2 - y_1, e_3 = z_2 - z_1$. These definitions, together with Eqs. (IV.1), yield the following governing equations for the deviations e_i :

$$\begin{aligned} \dot{e}_1 &= \mu e_3 - (1 + y_1^2)e_1, \\ \sigma \dot{e}_2 &= (1 + y_1^2)e_1, \\ \delta \dot{e}_3 &= -e_3. \end{aligned} \tag{IV.2}$$

We find the steady state by simply setting the right-hand side of (IV.2) to zero and solving the algebraic equations for e_1^*, e_2^* and e_3^* , where e_i^* represents the steady state value of e_i . The system exhibits a single steady state $(e_1^*, e_2^*, e_3^*) = (0, e_2^*, 0)$, where e_2^* is a constant that depends on the initial conditions.

We now examine the stability of the steady state by considering the function $v(e_1, e_2, e_3) = \frac{(1+y_1^2)\delta+1}{2(\delta\mu)^2}e_1^2 + \frac{1}{\delta\mu}e_1e_3 + e_3^2$ and showing that it is a Lyapunov function for (IV.2). For the steady state to be asymptotically stable, we have $v(e_1, e_2, e_3) > 0$ and $dv/dt < 0$ for e_i , and $v = 0$ and $dv/dt = 0$ only for $(e_1, e_2, e_3) = (e_1^*, e_2^*, e_3^*)$ [43]. The Lyapunov function v satisfies these conditions, since $v = ae_1^2 + be_1e_3 + ce_3^2 \geq 0$ if $4ac - b^2 = \frac{2(1+y_1^2)\delta+1}{(\delta\mu)^2} \geq 0$, which is fulfilled for all y_1 and $\delta \geq 0$. Hence, any solution of (IV.2) converges to this steady state over time, and any perturbation of the system from this steady state asymptotically decays to zero: $(e_1, e_2, e_3) \rightarrow (0, e_2^*, 0)$ as $t \rightarrow \infty$. Consequently, the pairs of variables (x_1, x_2) and (z_1, z_2) that define the differences e_1 and e_3 completely synchronize in the long-term limit, and since $e_1 \rightarrow 0$ as $t \rightarrow \infty$, the second equation of (IV.2) implies that $e_2 = y_2 - y_1 \rightarrow c$, where c is a constant that depends on the initial conditions of the full system (IV.1).

The constant c is a conserved quantity which, in contrast to Eqs. (III.1) considered in Sec. III, is not given directly by the initial conditions but evolves to its final value on approaching the asymptotic state and, hence, depends on the initial conditions in a nontrivial way. The value of

c corresponds to the synchronization manifold on which the long-term dynamics takes place. In contrast to the system considered in Sec. III, the schematic picture depicted in Fig. 4 holds only as $t \rightarrow \infty$. In the long-term limit, the state space is divided into infinitely many synchronization manifolds, each of them corresponding to a particular value of c . However, the initial condition is not necessarily contained in this manifold, as described above.

This analysis indicates that a new value of c is obtained for each new set of initial conditions, establishing a constant difference between the remaining pair of variables (y_1, y_2) . We can therefore substitute $y_2 = y_1 + c$ into the first subsystem and obtain a reduced system that can be further used to explore the extreme multistability for $t \rightarrow \infty$:

$$\begin{aligned} \dot{x}_1 &= \mu(\kappa + z_1) - x_1(1 + y_1^2), \\ \sigma y_1 &= x_1(1 + y_1^2) - y_1, \\ \delta z_1 &= (y_1 + c) - z_1, \end{aligned} \tag{IV.3}$$

This system is essentially the three-variable autocatalator model with the introduction of an additional parameter c , which depends on the initial conditions of the full system (IV.1) in a complex manner. The equivalence between the dynamical behavior as a function of the initial condition y_{02} for the full six-dimensional system and the behavior of the reduced three-dimensional system as a function of the conserved quantity c can be seen in a comparison of the bifurcation diagram in Fig. 7 to the initial conditions diagram in Fig. 6. The diagrams are in complete correspondence. We emphasize that Fig. 6 represents the long-term behavior for different initial conditions, which resembles a bifurcation diagram, while Fig. 7 is a bifurcation diagram in the mathematical sense, since c is a bifurcation parameter for the reduced system (IV.3).

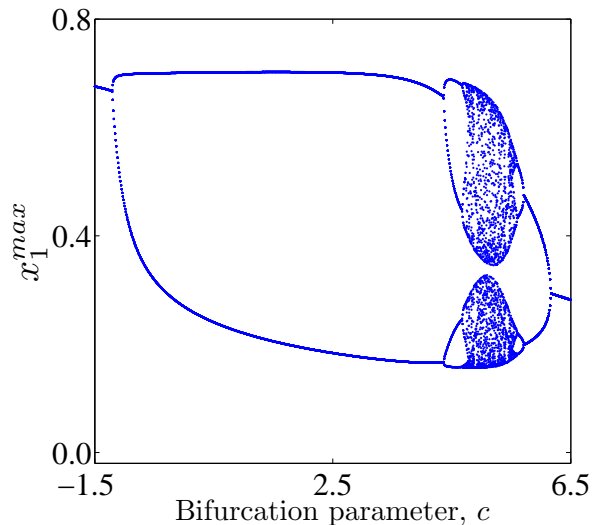


FIG. 7: (Color online) Bifurcation diagram of the reduced autocatalator model (IV.3) showing the maximum amplitude of x_1 as a function of the conserved quantity c .

Fig. 8 shows time series for chaotic and period-1 behavior of the long-term state for the full six-dimensional system. These plots demonstrate the nontrivial dependence of the final value of the conserved quantity c on the initial conditions. Because there is a relaxation of the system dynamics to the synchronization manifold corresponding to the conserved quantity $c = y_2 - y_1$, its value is not the same as the initial difference $y_{02} - y_{01}$.

Computing the Lyapunov exponents for the coupled six-variable autocatalator model (IV.1) reveals a pattern similar to that for Eqs. (III.1) considered in Sec. III. Due to the existence of the conserved quantity, we again find two zero Lyapunov exponents, as shown in Fig. 9.

B. Nonidentical coupled systems

We have assumed in our analysis of the coupled autocatalator systems in Sec. III and Sec. IV that the three-variable subsystems are identical, being described with the same set of parameters. This is, of course, a major assumption, since systems in nature are typically not identical but usually have at least some small mismatch in the parameters. The question arises whether extreme multistability is a robust phenomenon that also occurs when there is a mismatch in the parameters. For chemical systems, a mismatch in the parameters can be interpreted as a mismatch in the rate

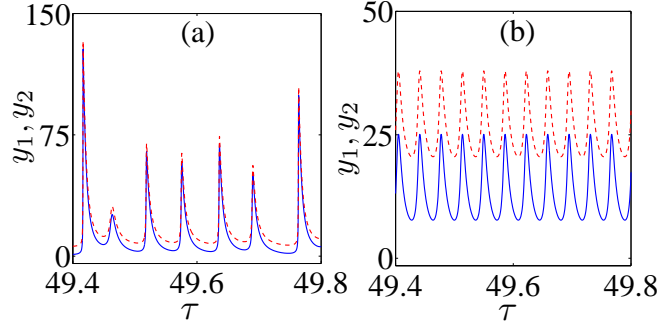


FIG. 8: (Color online) Time series illustrating the constant difference c between the dimensionless concentrations y_1 and y_2 for chaotic and period-1 behavior. (a) Chaotic behavior with $y_{02} = 7.2$, $c = 5.04$, and $y_{02} - y_{01} = 7.1$. (b) Period-1 behavior with $y_{02} = 15.0$, $c = 12.84$, and $y_{02} - y_{01} = 14.9$. Solid blue lines show y_1 and broken red lines show y_2 .

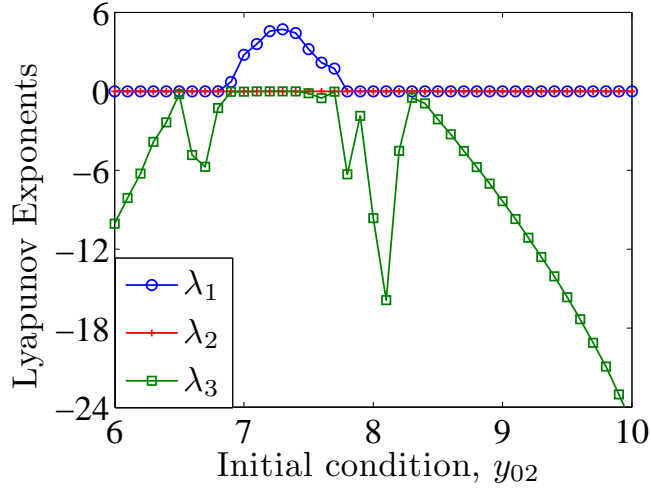


FIG. 9: (Color online) The three largest Lyapunov exponents of the coupled six-variable autocatalator model (IV.1) as a function of the initial condition y_{02} .

constants for the chemical reactions. We have examined parameter mismatches in the six-variable coupled autocatalator Eqs. (III.1) by varying κ , μ , σ and δ from 0 to 0.5% of their values. To obtain the mismatched parameter values, we scaled each of the dimensionless parameter groupings to reflect the effect of the individual rate constants lumped into the parameter. We first note that the bifurcations in the bifurcation diagrams shift with changing parameters such that the period

doubling cascade becomes smaller. For the larger parameter mismatches, only period-1 or chaotic solutions survive. We have examined the long-term dynamics exhibited with 0.01% and 0.05% parameter mismatches to determine whether extreme multistability is possible without identical subsystems. Our investigation suggests that the number of qualitatively different attractors may no longer tend to infinity as the parameter mismatch increases, as shown in Figs. 10 and 11. We conclude that extreme multistability is not fundamentally dependent on the coupled subsystems having identical parameters; however, the behavior is much more likely to occur when the subsystems are (or are almost) identical.

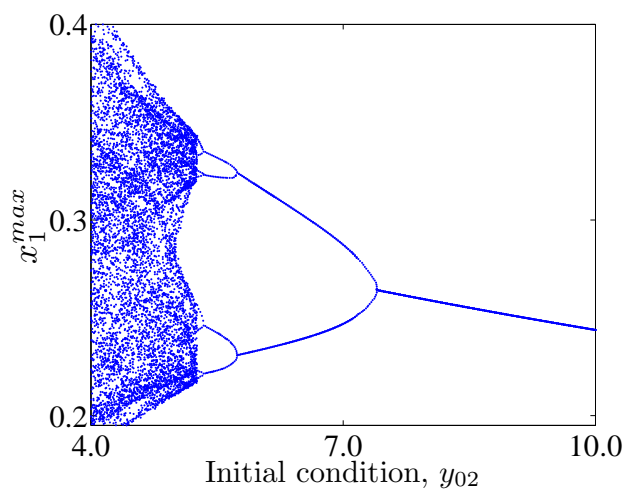


FIG. 10: (Color online) Long-term dynamics as a function of the initial condition y_{02} for the six-variable autocatalator Eqs. (III.1) with 0.01% parameter mismatch in the subsystem parameters.

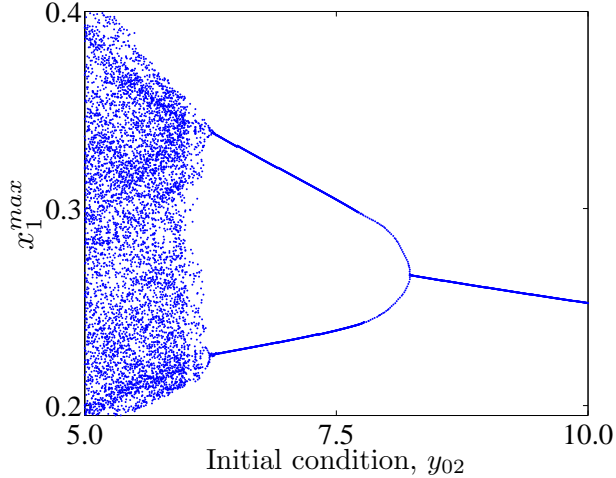


FIG. 11: (Color online) Long-term dynamics as a function of the initial condition y_{02} for the six-variable autocatalator Eqs. (III.1) with 0.05% parameter mismatch in the subsystem parameters.

V. DISCUSSION

We have demonstrated the phenomenon of extreme multistability using two coupled chemical systems. For two different couplings, the systems exhibit an infinite number of attractors as their asymptotic dynamical behavior. Depending on the initial conditions, many kinds of attractors, e.g. fixed points, periodic and chaotic orbits, are obtained. To explain this phenomenon, we have shown that extreme multistability is closely related to the emergence of a conserved quantity. The conserved quantity may appear due to a particular coupling scheme that gives rise to system variables that are no longer independent. In this case, the value of the conserved quantity is determined directly by the initial conditions. For another choice of the coupling, the conserved quantity emerges from the dynamics in the long-term limit. The latter case is more complex, as the conserved quantity appears only when the trajectory reaches the attractor.

The dynamical behavior of the coupled systems is characterized by two properties of extreme multistability: (i) The dynamics takes place on a complex manifold in state space which is determined by the value of a conserved quantity. In the absence of perturbations, the system trajectory remains on this manifold. Hence, in the limit $t \rightarrow \infty$, extreme multistability can be interpreted in terms of a division of the state space into infinitely many manifolds on which the dynamics takes place. (ii) Extreme multistability is accompanied by the appearance of a generalized synchroniza-

tion between the coupled subsystems. The emergence of a conserved quantity in the long-term limit allows for a model reduction of the coupled system Eqs. (IV.1). Since the dynamics for $t \rightarrow \infty$ takes place on a hypersurface in state space, which is determined by the value of the conserved quantity, the model system can be reduced to a new model in which the conserved quantity serves as a bifurcation parameter in the classical sense. This model reduction makes clear that infinitely many attractors occur, since the variation of this new bifurcation parameter gives rise to an infinite cascade of period doublings in the transition to chaos. Extreme multistability contains periodic orbits of all periods.

The existence of a conserved quantity resembles the dynamics of Hamiltonian systems. However, we emphasize that all of the systems considered here are dissipative and, hence, possess attractors, in contrast to Hamiltonian systems that only exhibit marginally stable orbits. The conserved quantity in Hamiltonian systems, e.g. energy, has a fixed value. This is also true for the system described by Eqs. (III.1); however, the conserved quantity for the system described by Eqs. (IV.1) emerges during the time evolution and its value is fixed only for $t \rightarrow \infty$.

Another issue to be addressed is the plausibility of our chemical models, since the corresponding reactions in the subsystems have the same rate constants. It is difficult to imagine two different chemical reactions having exactly the same rate constants, unless the corresponding chemical species were optical isomers of one another. However, we have demonstrated that a small variation in the rate constant values may be imposed without the disappearance of extreme multistability. It has been demonstrated in the coupled Lorenz system that a loss of extreme multistability occurs when the parameter mismatch is larger than $\simeq 0.1\%$ [4]. Hence, we conclude that extreme multistability is likely to occur only in almost identical coupled subsystems.

We have studied two different coupling schemes for the autocatalator model, both leading to extreme multistability. In order to generalize the approach, we attempted to determine a generic prescription for developing systems with infinitely many attractors. Such a generalization has remained elusive, however, in our studies. There are a variety of factors to take into account. These include symmetry and asymmetry, coupling both subsystems through a single variable, coupling both subsystems through two variables, selecting coupling variables from any of the equations involved in the system, etc. Considering these factors, we have developed a number of different couplings for the autocatalator system. Some of the coupled models exhibit extreme multistability, and some do not. We generally find that symmetry and asymmetry do not appear to be of major

importance for extreme multistability. We also find that coupling through a single variable fails to yield extreme multistability. Hence, we believe that the coupling should involve at least two variables.

Apart from the coupling, we may also try to generalize the notion of extreme multistability by considering the nature of the original subsystems. Here, we conjecture that a requirement for extreme multistability is chaos or chaotic subsystems. This is certainly a requirement for an infinite number of qualitatively different states, since the period doubling cascade to chaos is the characteristic that gives rise to this feature in all systems known to exhibit extreme multistability. We also carried out a search for an initial conditions dependence of the qualitative and quantitative states in coupled oscillatory systems, specifically the two-variable autocatalator; however, we have found no anomalous dynamical behavior.

As a last point, we address the robustness of extreme multistability against noise, which is inevitable in natural systems. For multistable systems possessing a large number of coexisting attractors, it has been shown that noisy dynamics can be viewed as a combination of two phases of motion, where the first phase is characterized by a motion around the attractor and the second phase corresponds to a jump from one attractor to another [44]. The duration of these two phases of motion is irregular, and the overall dynamics appears as a hopping process between different attractors. For systems exhibiting extreme multistability, we also observe this hopping as noise of a certain strength drives the system to move from one synchronization manifold to another one. Almost all perturbations lead to changes in the value of the conserved quantity and therefore to a change in the long-term dynamics. The exception, of course, is a perturbation in the values of the variables that preserves the value of the conserved quantity, for example, a perturbation that changes y_1 and y_2 equally in Eqs. (III.1) so that the value of the conserved quantity C remains the same. However, this argument does not apply to the system described by Eqs. (IV.1) because of its nontrivial relationship between the initial conditions and the final value of the conserved quantity c . Nevertheless, each system in any particular long-term final state possesses a manifold containing an infinite number of initial conditions that give rise to this final state attractor.

Extreme multistability is an unusual type of multistability behavior. It appears when two identical systems are coupled in a particular way so that a conserved quantity emerges. While the phenomenon has not been shown to be general in the usual sense, we now know that it appears in chemical model systems as well as in mathematical models such as the coupled Lorenz equations.

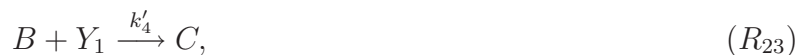
Although the chemistry of these models is somewhat complex, each step is reasonable and follows from simple mass action kinetics. We are convinced that many systems exhibiting chaotic behavior will exhibit extreme multistability when two such systems are appropriately coupled.

VI. ACKNOWLEDGEMENT

The authors would like to thank Brian Hunt, Arkady Pikovsky, Eckehard Schöll, and Binoy Goswami for illuminating discussions. K.S. thanks the National Science Foundation (CHE-0809058) for support of this research.

VII. APPENDIX

The chemical coupling giving rise to Eqs. (IV.1) is described here. The model involves the conversion of a chemical precursor A to a final product E through six chemical intermediates X_i , Y_i and Z_i ($i = 1, 2$). This occurs in two subsystems with an intermediate from each subsystem involved in the other subsystem, comparable to the model (R_7)-(R_{18}) described by Eqs. (III.1). In the course of the conversion, two products C and D are formed that do not participate in the dynamics, as well as the main product E . We therefore do not include the time evolution of these species in deriving system (VII.1) below. Defining k_i ($i = 0, 1, 2, 4, 3, 5$), k'_4 and k''_4 as the rate constants, the chemical representation of the model follows:





The concentrations of A and B are assumed to be constant at A_0 and B_0 , and we assume that $k''_4 \gg k'_4 B_0 = k_4$. Reaction (R_{22}) of the first subsystem describes an autocatalytic process, in which Y_1 catalyzes its own production. Since Y_1 is produced through autocatalysis in the first subsystem and is used to produce Y_2 in the second subsystem, we can also imagine an indirect autocatalysis occurring in the fourth equation of the second subsystem (R_{29}) . Unlike the individual three-variable subsystems, each of which has simple feedback loops, there are more complex feedback loops in the coupled system. For example, Z_1 and Z_2 are produced in reaction (R_{24}) and fed back into the system through reactions (R_{20}) and (R_{27}) , respectively, to catalyze the production of X_1 from A and the production of X_2 from A . These feedbacks contribute to the complex dynamics. It is worth noting that while B is constant with the value B_0 , C is generated in reaction (R_{23}) of the first subsystem and rapidly consumed in reaction (R_{30}) of the second subsystem. The rate of reaction (R_{30}) is therefore determined by the rate of reaction (R_{23}) . Consequently, we use $k_4 Y_1 = k'_4 B_0 Y_1$ instead of $k''_4 C Y_2$ in the corresponding model. This feedback also contributes to the coupling of the two subsystems. For the remaining modes of coupling, notice that the first subsystem is also coupled to the second subsystem through Y_2 in the sixth reaction of the first subsystem (R_{24}) , while the second subsystem is coupled to the first subsystem through Y_1 in the fourth equation of the second subsystem (R_{29}) .

Let A_0 , $[X_1]$, $[Y_1]$, $[Z_1]$, $[X_2]$, $[Y_2]$ and $[Z_2]$ be the concentrations of A , X_1 , Y_1 , Z_1 , X_2 , Y_2 and Z_2 respectively. Then using the law of mass action we write the following system of first-order

ordinary differential equations for the above model:

$$\begin{aligned}
[\dot{X}_1] &= k_0 A_0 + k_1 A_0 [Z_1] - k_2 [X_1] - k_3 [X_1] [Y_1]^2, \\
[\dot{Y}_1] &= k_2 [X_1] + k_3 [X_1] [Y_1]^2 - k_4 [Y_1], \\
[\dot{Z}_1] &= k_4 [Y_1] - k_5 [Z_1], \\
[\dot{X}_2] &= k_0 A_0 + k_1 A_0 [Z_2] - k_2 [X_2] - k_3 [X_2] [Y_1]^2, \\
[\dot{Y}_2] &= k_2 [X_2] + k_3 [X_2] [Y_1]^2 - k_4 [Y_1], \\
[\dot{Z}_2] &= k_4 [Y_2] - k_5 [Z_2].
\end{aligned} \tag{VII.1}$$

We note that the law of mass action kinetics is obeyed; however, unlike model (R_7) - (R_{18}) giving rise to Eqs. (III.1), model (R_{19}) - (R_{31}) giving rise to Eqs. (VII.1), from which Eqs. (IV.1) follow, includes chemical steps that may not be plausible. Nevertheless, we present this model to explore the unusual extreme multistability involving an evolution of the conserved quantity.

-
- [1] J. Guckenheimer and P. Holmes, *Nonlinear Oscillations, Dynamical systems, and Bifurcations of Vector Fields* (Springer Verlag, Berlin, Heidelberg, New York, 1986).
- [2] E. Ott, *Chaos in Dynamical Systems* (Cambridge University Press, Cambridge, 1992).
- [3] B. Goswami and A. Pisarchik, “Controlling multistability by small perturbations,” *Int. J. Bifurcation & Chaos* **18**, 1645–1673 (2008).
- [4] U. Feudel, “Complex dynamics in multistable systems,” *Int. J. Bifurcation & Chaos* **18**, 1607–1626 (2008).
- [5] V. Balzani, A. Credi, and M. Venturi, *Molecular Devices and Machines* (Wiley-VCH Verlag GmbH and Co. KGaA, 2008), second edition.
- [6] F. Arecchi, R. Meucci, G. Puccioni, and J. Tredicce, “Experimental evidence of subharmonic turbulence in a q-switched gas laser,” *Phys. Rev. Lett.* **49**, 1217–1220 (1982).
- [7] C. Masoller, “Noise-induced resonance in delayed feedback systems,” *Phys. Rev. Lett.* **88**, 034102 (2002).
- [8] J. Kastrop, H. Grahn, K. Ploog, F. Pregel, A. Wacker, and E. Schöll, “Multistability of the current-voltage characteristics in doped GaAs superlattices,” *Appl. Phys. Lett.* **65**, 1808–1810 (1994).
- [9] G. Schwarz, C. Lehmann, and E. Schöll, “Self-organized symmetry-breaking current filamentation and multistability in Corbino disks,” *Phys. Rev. B* **61**, 10194–10200 (2000).
- [10] N. Ganapathisubramanian and K. Showalter, “Bistability, mushrooms, and isolas,” *J. Chem. Phys.* **80**, 4177–4184 (1984).
- [11] P. Marmillot, M. Kaufman, and J.-F. Hervagault, “Multiple steady states and dissipative structures in a circular and linear array of three cells: Numerical and experimental approaches,” *J. Chem. Phys.* **95**, 1206–1214 (1991).
- [12] J. Foss, A. Longtin, B. Mensour, and J. Milton, “Multistability and delayed recurrent loops,” *Phys. Rev. Lett.* **76**, 708–711 (1996).
- [13] J. Huisman and F. Weissing, “Fundamental unpredictability in multispecies competition,” *Am. Nat.* **157**, 488–494 (2001).
- [14] U. Feudel, C. Grebogi, B. R. Hunt, and J. A. Yorke, “A map with more than 100 coexisting low-period periodic attractors,” *Phys. Rev. E* **54**, 71–81 (1996).

- [15] B. Goswami, “Multiple attractors in the self-similar bifurcation-structure,” *Rivista del Nuovo Cimento* **23**, 1–115 (2005).
- [16] K. Kaneko, ed., *Theory and applications of coupled map lattices* (Wiley, New York, 1993).
- [17] A. Pikovsky, O. Popovych, and Y. Maistrenko, “Resolving clusters in chaotic ensembles of globally coupled identical oscillators,” *Phys. Rev. Lett.* **87**, 044102 (2001).
- [18] V. Astakhov, A. Shabunin, W. Uhm, and S. Kim, “Multistability formation and synchronization loss in coupled h enon maps: Two sides of the single bifurcational mechanism,” *Phys. Rev. E* **63**, 056212 (2001).
- [19] A. Balanov, N. Janson, and E. Sch oll, “Delayed feedback control of chaos: Bifurcation analysis,” *Phys. Rev. E* **71**, 016222 (2005).
- [20] C. Masoller and N. Abraham, “Stability and dynamical properties of the coexisting attractors of an external-cavity,” *Phys. Rev. A* **57**, 1313–1322 (1998).
- [21] B. Krauskopf, “Semiconductor lasers as dynamical systems,” in F. Dumortier, D. Roose, and A. Vanderbauwhede, eds., “Trends in Dynamical Systems,” 33–45 (Handelingen van de Koninklijke Vlaamse Academie van Belgie, 2006).
- [22] H. Sun, S. Scott, and K. Showalter, “Uncertain destination dynamics,” *Phys. Rev. E* **60**, 3876–3880 (1999).
- [23] P. Gray and S. K. Scott, *Chemical Oscillations and Instabilities. Non-linear Chemical Kinetics* (Oxford University Press, New York, 1994).
- [24] S. K. Scott, *Chemical Chaos* (Oxford University Press, New York, 1991).
- [25] M. Orban and I. R. Epstein, “Complex periodic and aperiodic oscillation in the chlorite-thiosulfate reaction,” *J. Phys. Chem.* **86**, 3907–3910 (1982).
- [26] I. Nagypal and I. R. Epstein, “Fluctuations and stirring rate effects in the chlorite-thiosulfate reaction,” *J. Phys. Chem.* **90**, 6285–6292 (1986).
- [27] J. Wang, H. Sun, S. K. Scott, and K. Showalter, “Uncertain dynamics in nonlinear chemical reactions,” *Phys. Chem. Chem. Phys.* **5**, 5444–5447 (2003).
- [28] V. Petrov, S. Scott, and K. Showalter, “Mixed-mode oscillations in chemical systems,” *J. Chem. Phys.* **97**, 6191–6198 (1992).
- [29] A. Milik, P. Szmolyan, H. Loffelmann, and E. Groller, “Geometry of mixed-mode oscillations in the 3-D autocatalator,” *Int. J. Bifurcation Chaos* **8**, 505–519 (1998).

- [30] I. Z. Kiss and V. Gaspar, “Controlling chaos with artificial neural network: Numerical studies and experiments,” *J. Phys. Chem. A* **104**, 8033–8037 (2000).
[Online Version](#)
- [31] Y. Li, X. Liao, C. Li, T. Huang, and D. Yang, “Impulsive synchronization and parameter mismatch of the three-variable autocatalator model,” *Phys. Lett. A* **366**, 52 – 60 (2007).
[Online Version](#)
- [32] C. Piccardi, “Parameter estimation for systems with peak-to-peak dynamics,” *Int. J. Bifurcation Chaos* **18**, 745–753 (2008).
- [33] J. Guckenheimer, “Singular Hopf Bifurcation in Systems with Two Slow Variables,” *SIAM J. Appl. Dyn. Syst.* **7**, 1355–1377 (2008).
- [34] B. Peng, S. K. Scott, and K. Showalter, “Period doubling and chaos in a three-variable autocatalator,” *J. Phys. Chem.* **94**, 5243–5246 (1990).
- [35] P. Gray and S. K. Scott, “Autocatalytic reactions in the isothermal continuous stirred tank reactor: isolas and other forms of multistability,” *Chem. Engng. Sci* **39**, 29–43 (1983).
- [36] J. H. Merkin, D. J. Needham, and S. K. Scott, “On the creation, growth and extinction of oscillatory solutions for a simple pooled chemical reaction scheme,” *S.I.A.M Journal on Applied Applied Mathematics* **47**, 1040–1060 (1987).
- [37] L. K. Forbes and C. A. Holmes, “Limit cycle behavior in a model for chemical reaction: the cubic autocatalator,” *Journal of Engineering Mathematics* **24**, 179–189 (1990).
- [38] B. Peng, V. Petrov, and K. Showalter, “Controlling chemical chaos,” *J. Phys. Chem.* **95**, 4957–4959 (1991).
- [39] E. Hairer and G. Wanner, *Solving Ordinary Differential Equations II: Stiff and Differential-Algebraic Problems* (Springer-Verlag, Berlin, Heidelberg, New York, 1996), 2nd edition.
- [40] J. Milnor, “On the concept of attractor,” *Commun. Math. Phys.* **99**, 177 – 195 (1985).
- [41] A. Pikovsky, M. Rosenblum, and J. Kurths, *Synchronisation* (Cambridge University Press, Cambridge, 2000).
- [42] L. Pecora and T. Carroll, “Synchronization in chaotic systems,” *Phys. Rev. Lett.* **64**, 821–824 (1990).
- [43] D. W. Jordan and P. Smith, *Nonlinear Ordinary Differential Equations. An Introduction to Dynamical Systems* (Oxford University Press, Oxford, UK, 1999), 3rd edition.
- [44] U. Feudel and C. Grebogi, “Multistability and the control of complexity,” *CHAOS* **7**, 597–604 (1997).

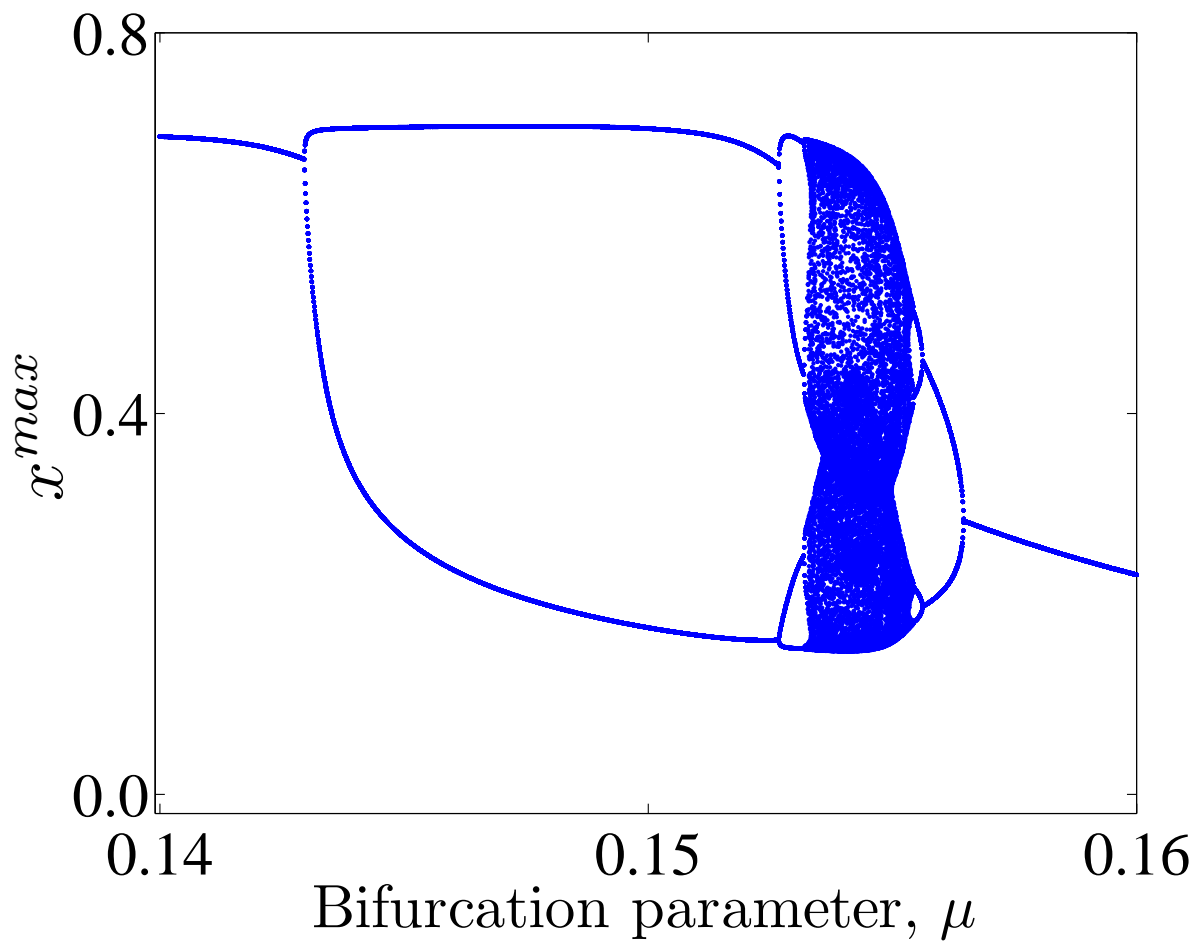
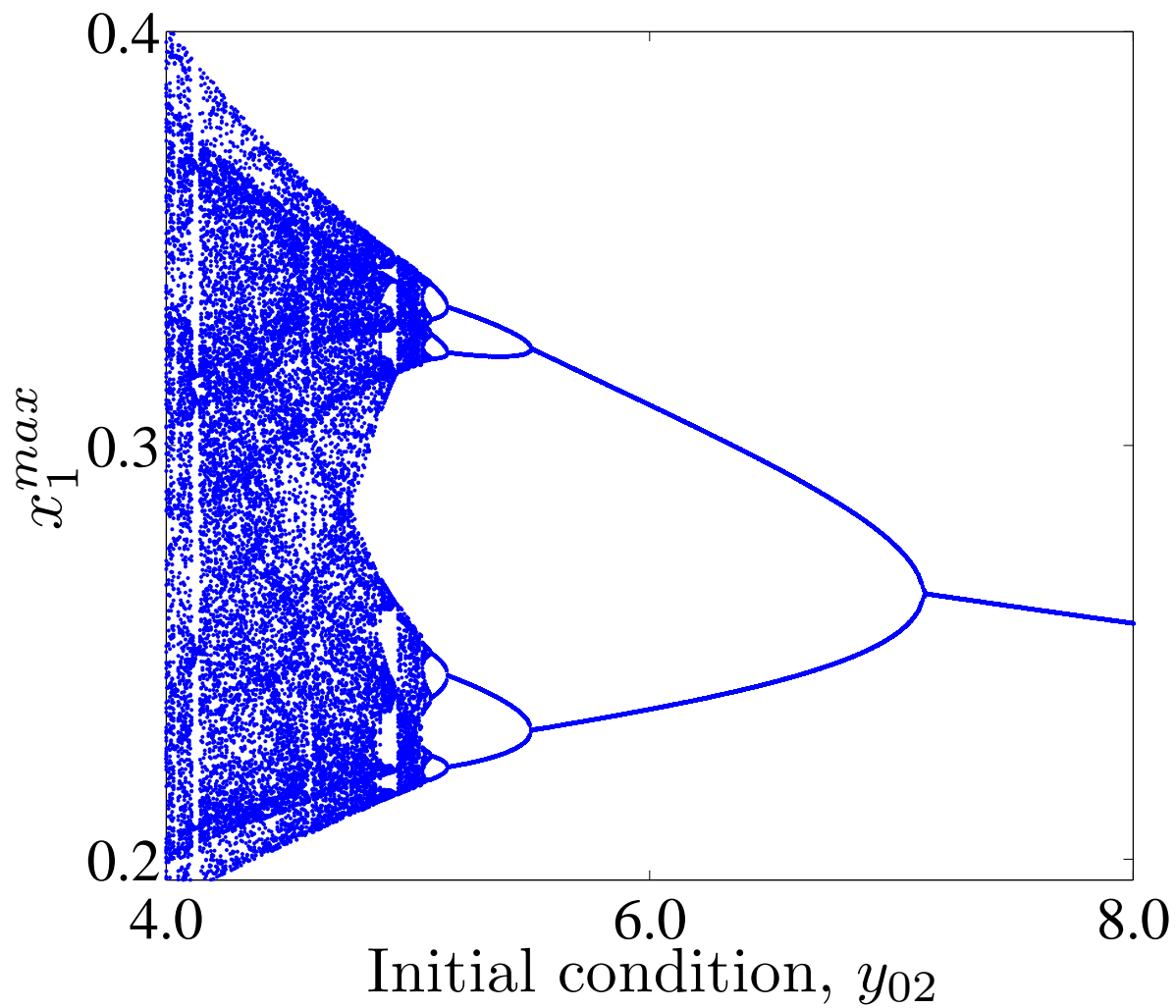


Figure 1 EY10493 22Feb2011



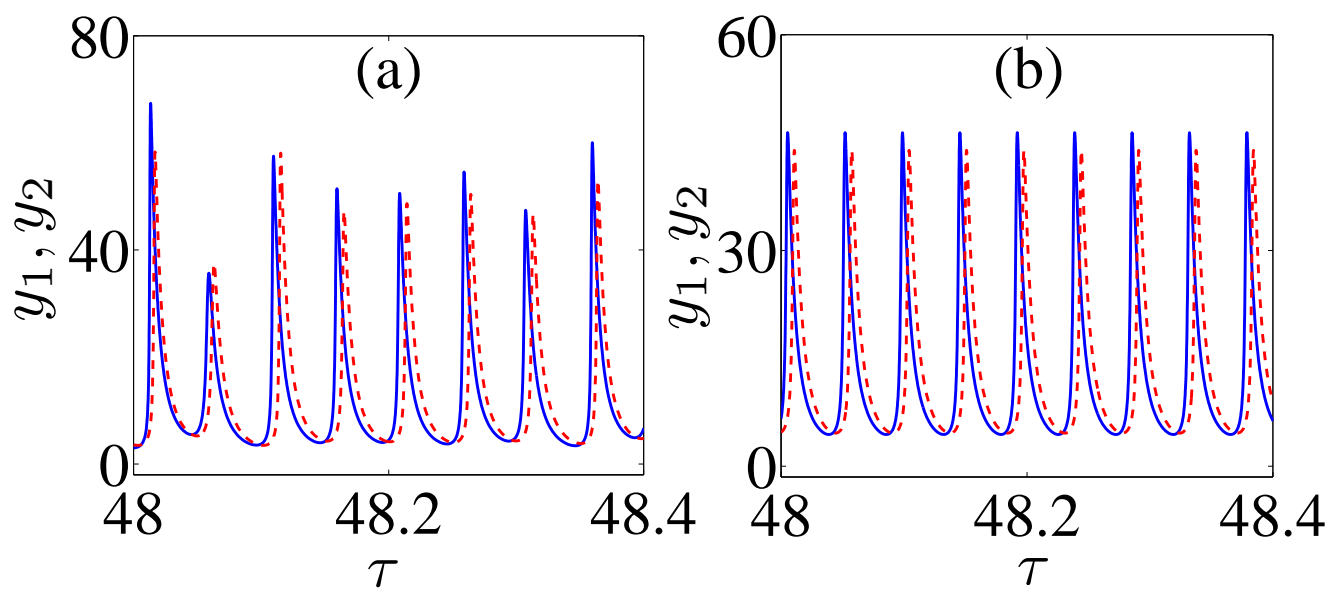


Figure 3

EY10493

22Feb2011

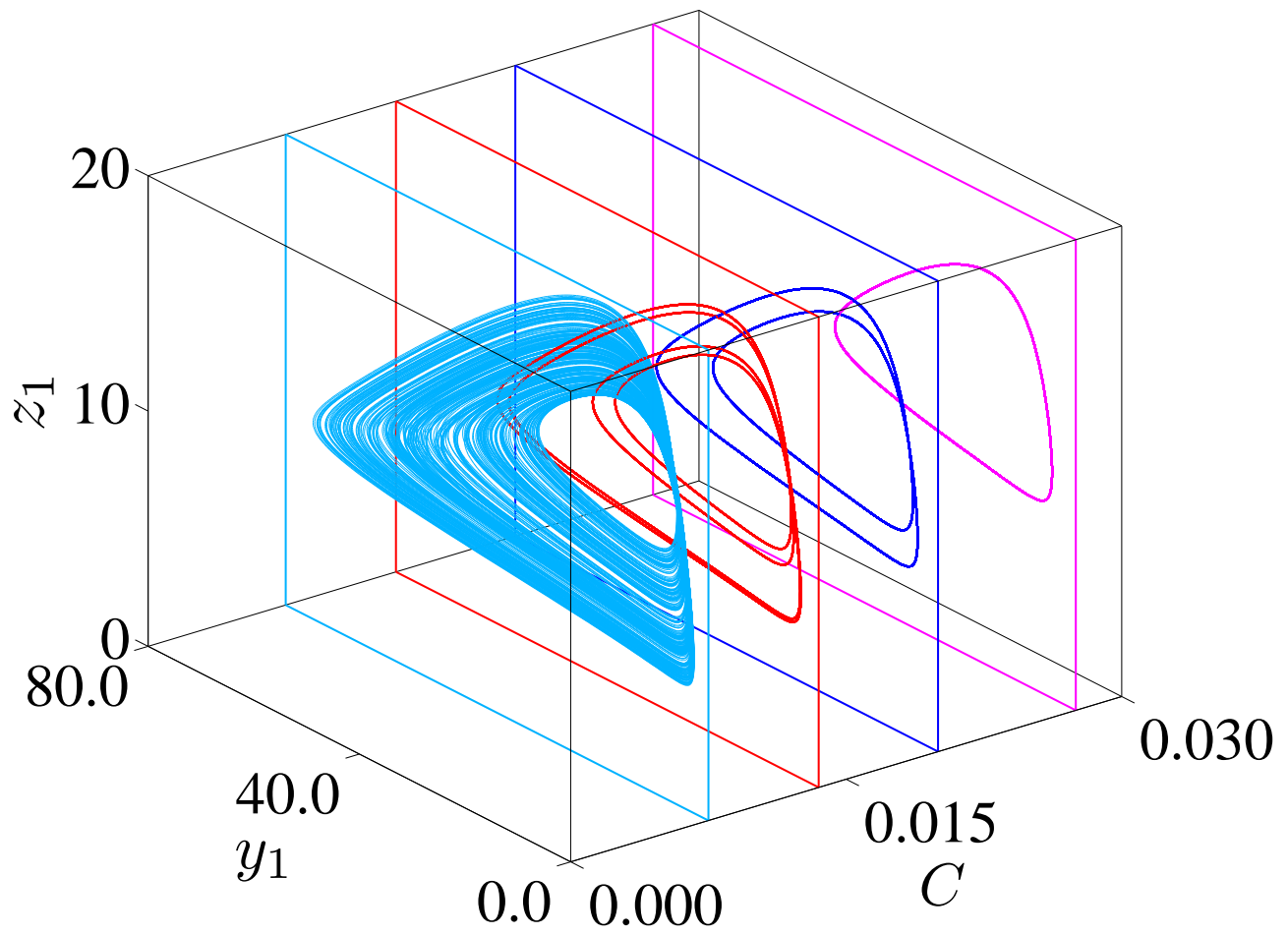


Figure 4

EY10493

22Feb2011

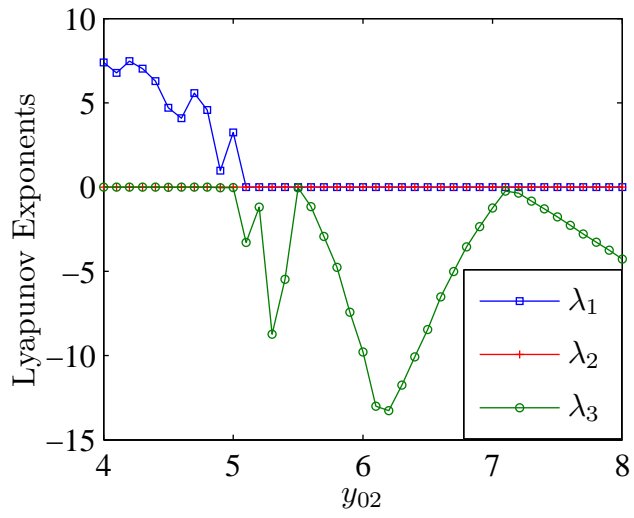


Figure 5 EY10493 22Feb2011

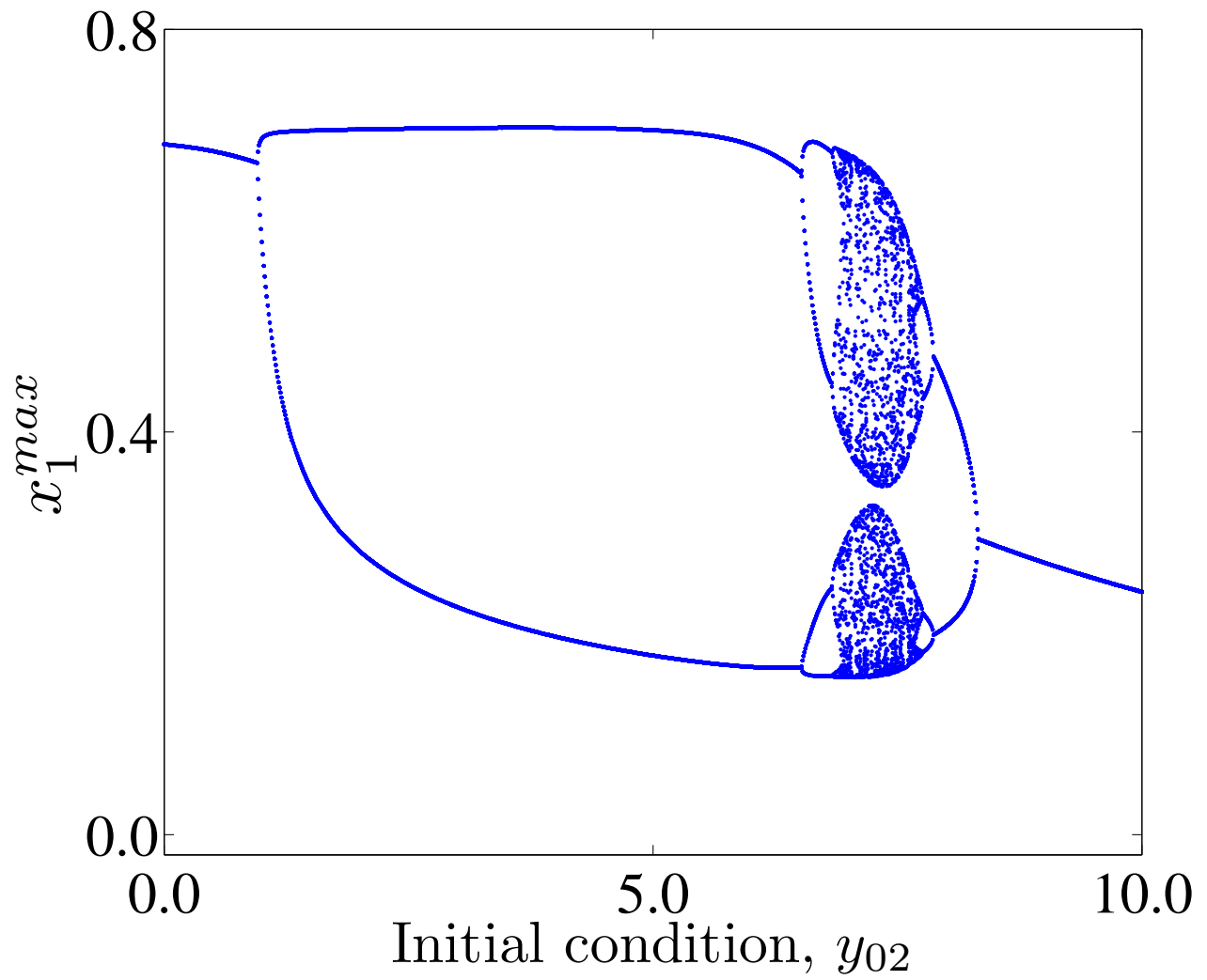


Figure 6 EY10493 22Feb2011

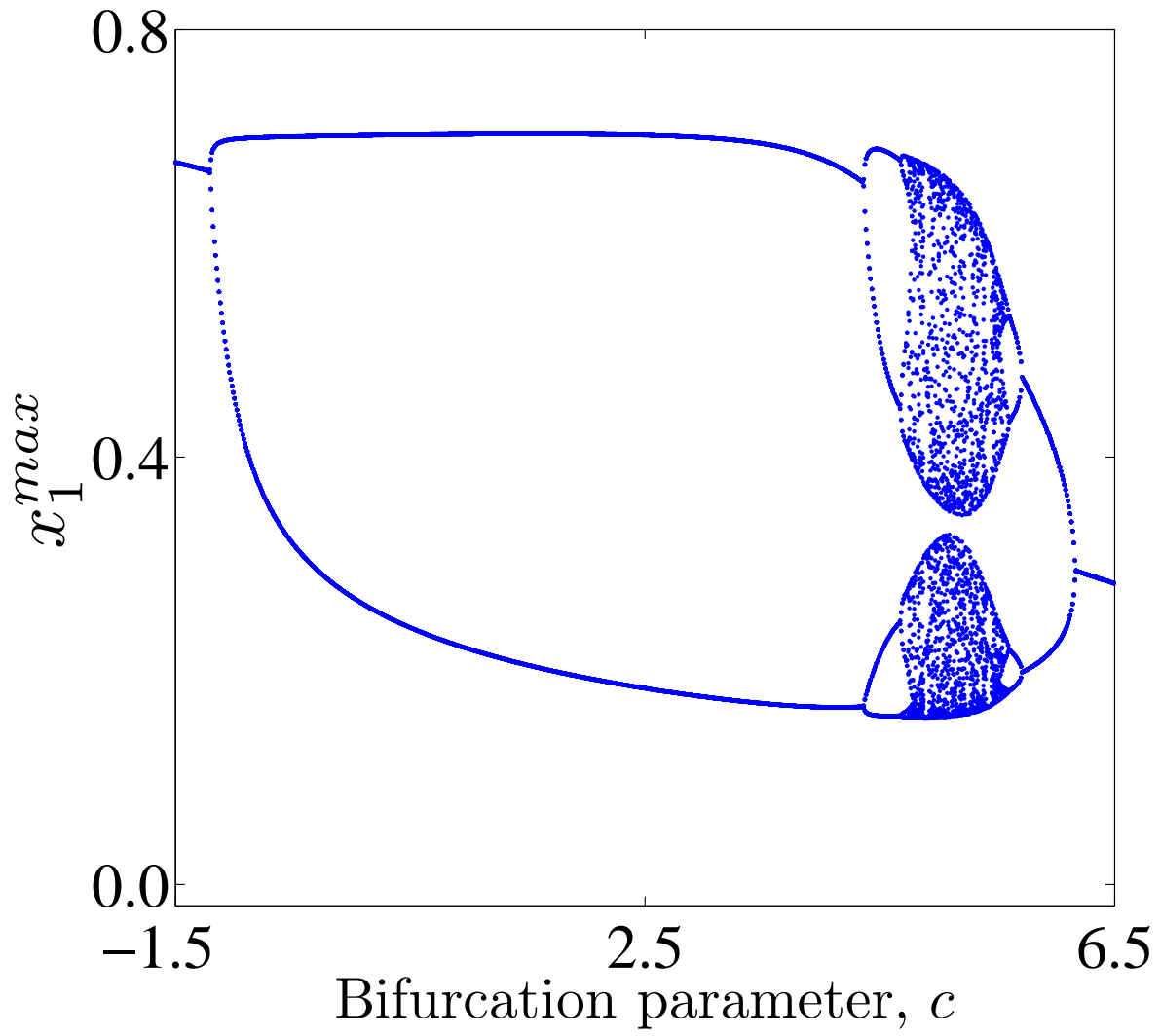


Figure 7 EY10493 22Feb2011

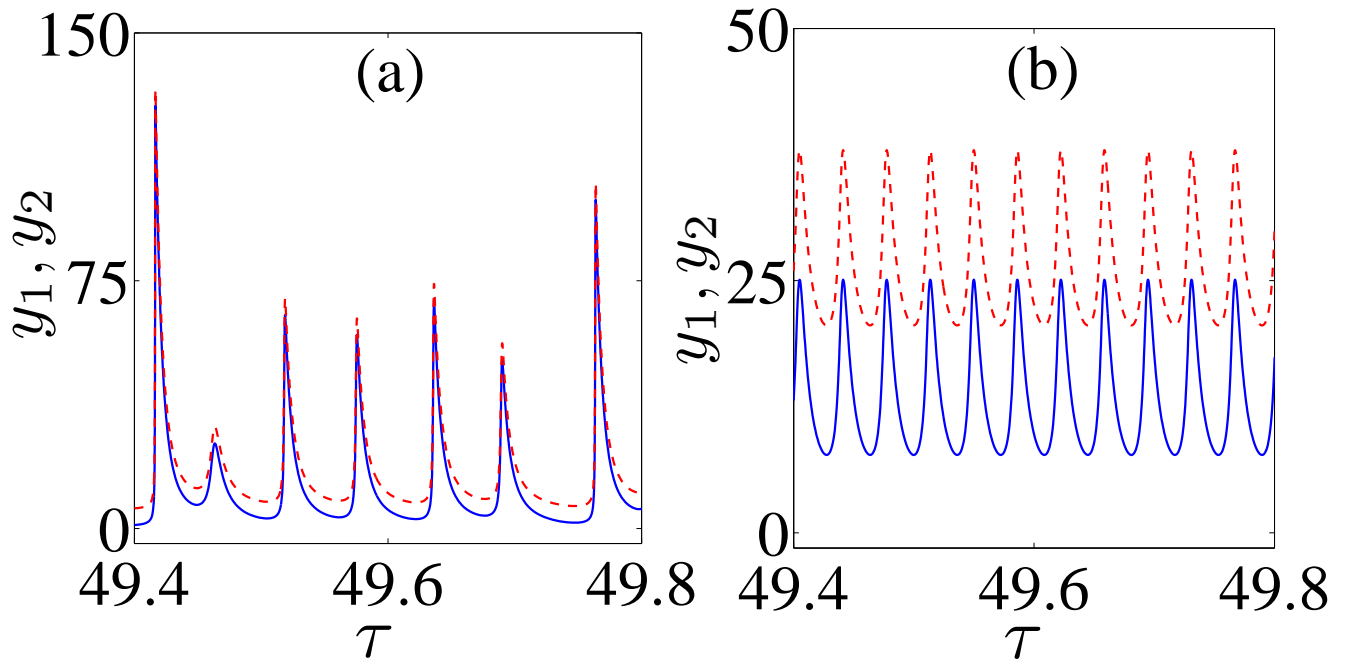


Figure 8

EY10493

22Feb2011

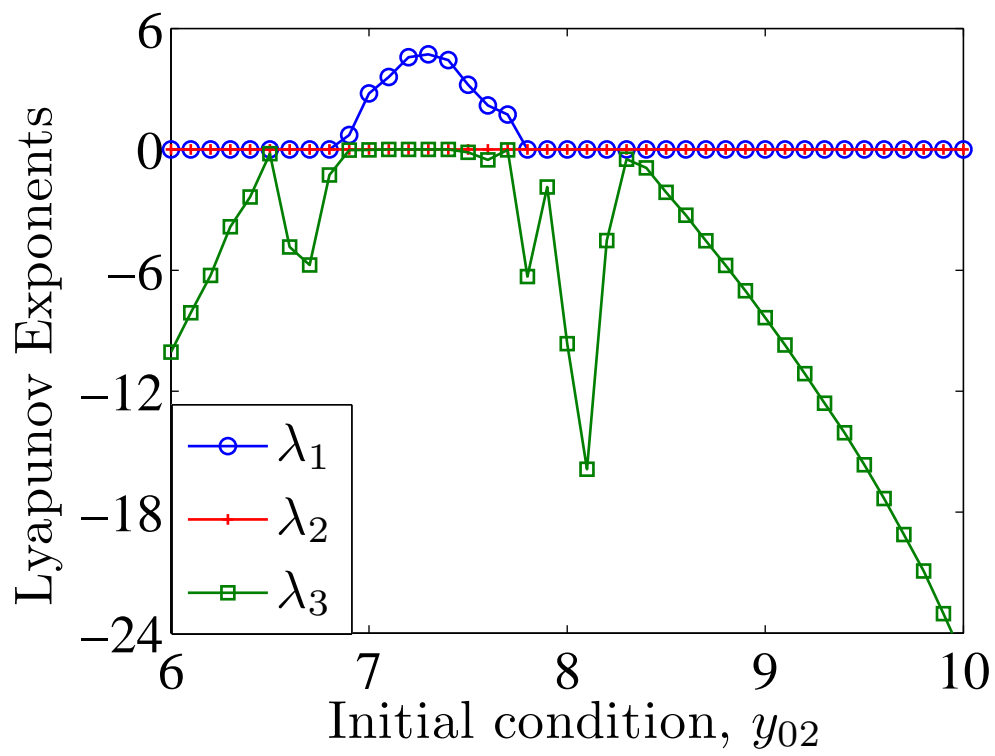


Figure 9

EY10493

22Feb2011

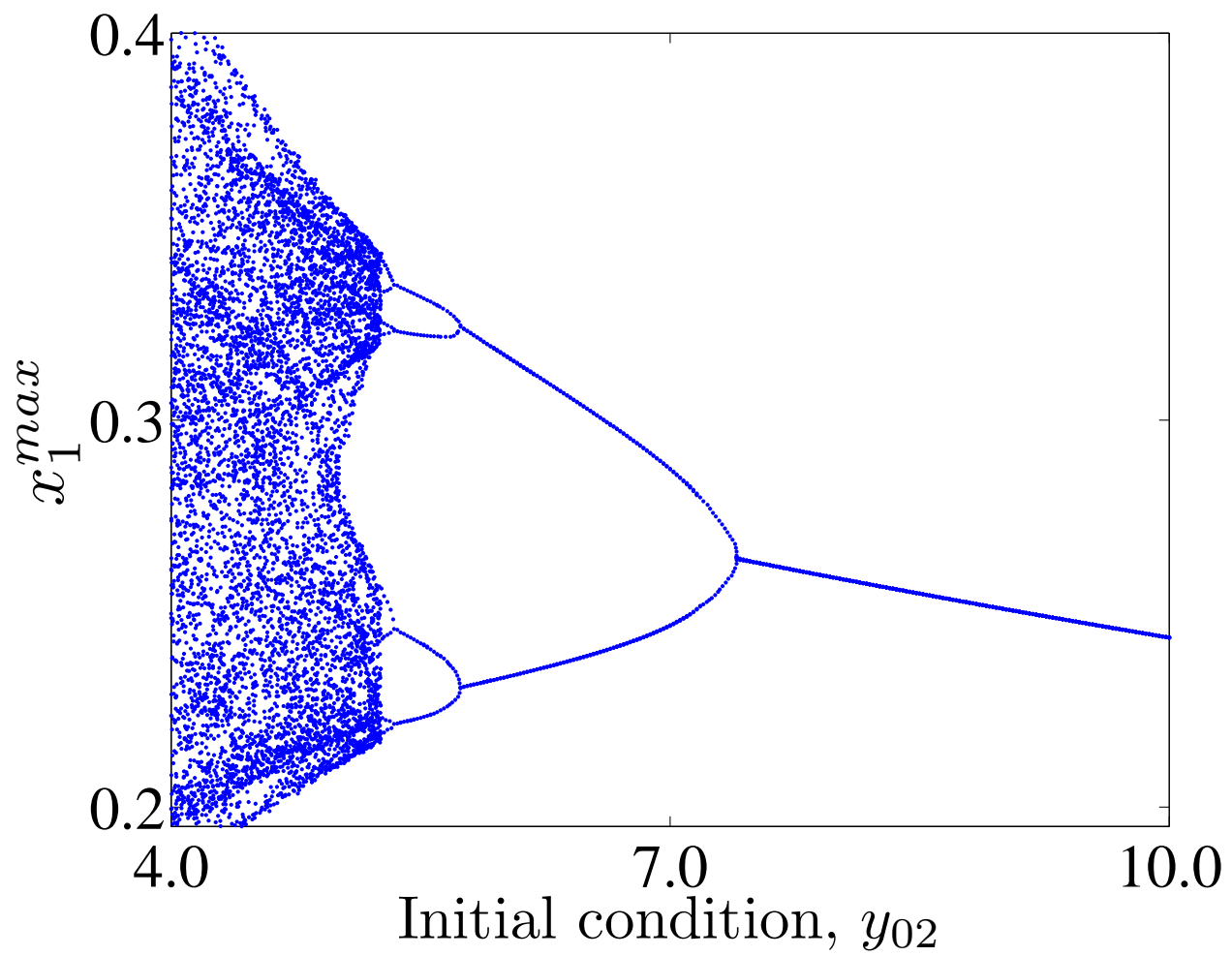


Figure 10 EY10493 22Feb2011

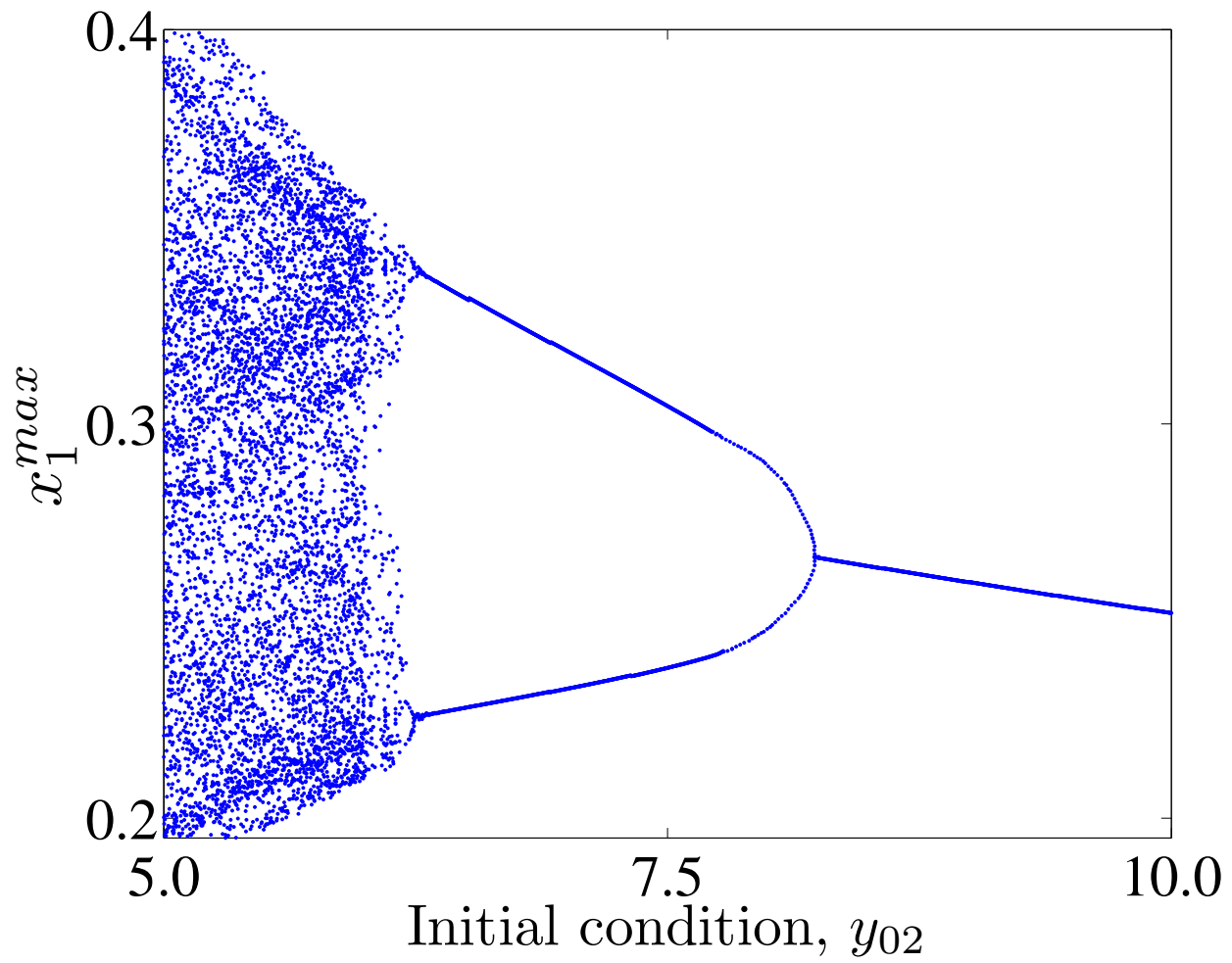


Figure 11 EY10493 22Feb2011